

## **General Disclaimer**

### **One or more of the Following Statements may affect this Document**

- This document has been reproduced from the best copy furnished by the organizational source. It is being released in the interest of making available as much information as possible.
- This document may contain data, which exceeds the sheet parameters. It was furnished in this condition by the organizational source and is the best copy available.
- This document may contain tone-on-tone or color graphs, charts and/or pictures, which have been reproduced in black and white.
- This document is paginated as submitted by the original source.
- Portions of this document are not fully legible due to the historical nature of some of the material. However, it is the best reproduction available from the original submission.

**NASA TECHNICAL  
MEMORANDUM**

**NASA TM X-73631**

(NASA-TM-X-73631) PROBE STUDIES IN A  
MODIFIED PENNING DISCHARGE (NASA) 15 p HC  
A02/MF A01 CSCI 20I

N78-15905

Unclass

G3/75 57789

NASA TM X-73631

**PROBE STUDIES IN A MODIFIED PENNING DISCHARGE**

by Chitra Sen  
Lewis Research Center  
Cleveland, Ohio 44135

TECHNICAL PAPER presented at the  
Eighteenth Annual Meeting on Plasma Physics  
sponsored by the American Physical Society  
San Francisco, California, November 14-18, 1976



# PROBE STUDIES IN A MODIFIED PENNING DISCHARGE

by Chitra Sen

National Aeronautics and Space Administration  
Lewis Research Center  
Cleveland, Ohio

## ABSTRACT

The axial and radial floating potential distribution in a modified Penning discharge have been studied at different values of the background pressure, discharge voltage, and magnetic field. An array of small disc probes arranged radially with their planes perpendicular to the magnetic field and movable along the axial direction was inserted in the plasma through one open end of the magnetic mirror system. Results show that depending on the operating conditions, the discharge can undergo different mode transitions in which the plasma can sustain different floating potentials in the radial as well as in the axial directions. Preliminary results of measurement, using rf probes in the modified Penning discharge plasma are also discussed.

## INTRODUCTION

The modified Penning discharge has been studied by Roth<sup>1</sup> (1966) in connection with the presence of hot ions<sup>1,2</sup> (1966, 1973a), measuring their energy distribution<sup>3,4</sup> (1969, 1973b) and searching for their origin<sup>5,6</sup> (1971, 1973c). Yet, many of the basic physical processes such as mechanisms of particle transport are still unknown in such a discharge.

The modified Penning discharge is characterized by the presence of strong crossed electric and magnetic fields. The electric field acting on the plasma plays an important role in determining the particle transport and the confinement of the plasma. It is, therefore, desirable to have a knowledge of the potential distribution within the plasma. The present study on the modified Penning discharge consists of two parts. Part one deals with the study of the potential distribution within the plasma and part two deals with the study of plasma parameters by rf impedance probe.

A number of methods are available for studying the potential distribution within a plasma but the more desirable such as ion beam probing method<sup>7</sup> are major undertakings. Though subject to criticism, Langmuir probes because of their simplicity and ready availability have been used in the past years<sup>8,9</sup> (Roth 1976, Nishida and Hirose 1976) for measuring the floating potential distribution in a magnetized plasma. In this present study the radial and axial potential distributions within the

modified Penning discharge plasma have been measured under different operating conditions using floating probes. The pressure of the discharge was varied from  $4 \times 10^{-6}$  to  $2 \times 10^{-4}$  torr, the anode voltage was varied from 800 volts to 24 kilovolts and the magnetic field was varied from 0.42 to 1.12 Tesla at the magnetic mirror position. In this range of operating conditions, the discharge underwent mode transitions which exhibited substantially different potential distributions within the plasma.

RF impedance probe has been successfully applied by Sen and Basu<sup>10</sup> (1973) and by Basu and Sen<sup>11</sup> (1975) in determining the electron density and electron temperature in glow and arc discharge plasmas, in absence of a magnetic field. The same method has been applied in the modified Penning discharge plasma in which the impedance of a disc probe with its plane perpendicular to the magnetic field has been measured for different bias voltages. The result was then computed to yield the local values of the electron temperature and electron density of the plasma. For the sake of comparison, the corresponding electron temperature and density calculated from the d.c. probe characteristics are also being measured.

## EXPERIMENT

Figure 1 shows an isometric cutaway drawing of a modified Penning discharge in a superconducting magnetic mirror facility. The system is installed in a vacuum tank of 0.915 meter in diameter and 1.83 meters long. Three 25.4 centimeters diameter glass viewports are located on both sides of the tank, and there are two end viewports on the axis. The superconducting magnet system used in this experiment consists of a pair of 18 centimeter i.d. superconducting coils with an inside diameter of 17 centimeters arranged in a magnetic mirror configuration with a mirror ratio of  $B_{\min}/B_{\max} = 0.38$ . The anode consists of a pair of water-cooled rings, 15.2 centimeters in diameter and separated axially by 2.5 centimeters, placed at the midplane of the magnetic mirror system. This was operated at a positive potential of up to 24 kilovolts. The grounded superconducting magnet dewars acted as the cathode of the discharge. The magnetic field at the mirror throat was varied from 0.42 to 1.12 Tesla in this experiment. The operating gas was deuterium and was used in the pressure range of  $4 \times 10^{-6}$  to  $2 \times 10^{-4}$  torr.

An array of five disc probes, each 1 mm in diameter and spaced on 1 centimeter centers in the radial direction from discharge axis, was used in determining the floating potential distribution. The probe system was introduced from one open end of the magnetic mirror system and was movable in the axial direction. The floating potential of each of the probes determined by the zero current in the probe circuit was measured.

Figure 2 shows schematically the rf impedance probe measurement of the modified Penning discharge plasma. The probe is a large disc of 1 centimeter in diameter. It is connected coaxially with the RX-meter

through a blocking capacitor. Such a probe with rather large area was chosen for reducing, as far as possible, the inaccuracies in the measurements of its rf impedance and also for making the unidimensional analysis<sup>12</sup> (Basu and Sen, 1967) valid. The sides and the back of the probe were insulated and shielded from the plasma. The d.c. bias to the probe was given from a power supply through a rf rejection circuit. The ammeter in the probe bias circuit measures the probe d.c. current corresponding to any bias voltage.

The impedance of the probe for a frequency  $\omega \ll \omega_p$  is just the impedance of the probe sheath, which is a parallel combination of capacitance and resistance. This impedance has been measured by the RX-meter. By changing the bias of the probe the corresponding change in the probe sheath impedance was measured from which the probe sheath thickness and hence the electron temperature and electron density was calculated<sup>13</sup> (Sen, Ph.D. Thesis, 1975). For each bias voltage the corresponding d.c. probe current was also noted.

## RESULTS

Figure 3 shows a typical I-V characteristic of the modified Penning discharge taken at a magnetic field of 1.12 Tesla at the mirror throat. The pressure was varied from  $4 \times 10^{-6}$  to  $2.1 \times 10^{-4}$  torr, and the discharge voltage was varied from 0.8 to 24 kilovolts. In this operating range the behavior of the discharge could be classified into three broad categories.

### (a) Low Resistance Mode

Transition to this mode of operation takes place approximately at a pressure above  $10^{-4}$  torr and are shown by the upper left curves of figure 3. This mode is characterized by high discharge current and low discharge voltage. The plasma is very luminous and has a more or less Maxwellian velocity distribution as determined by the Langmuir probe characteristics. The plasma in this case floats at a high potential which may be a considerable fraction of the anode voltage on the axis which then increases monotonically in the radial direction. Figure 4 shows the radial distribution of the floating potential in the low resistance mode for different anode voltages, taken at the mirror throat position. While there is considerable potential drop in the radial direction, it remains almost constant along the axis, as shown in figure 5.

### (b) High Resistance Mode

This mode of operation is characterized by high discharge voltage and low discharge current, and are represented by the lower right curves of figure 3. Transition to this mode takes place approximately at pressures below  $6 \times 10^{-5}$  torr for deuterium. The plasma in this mode of oper-



ation is dim and has a Maxwellian electron velocity distribution. (As determined by the linearity of the  $\ln I_e - V_p$  of Langmuir probe characteristics.)

Figure 6 shows the radial floating potential distribution for the high resistance mode taken at the mirror throat for different anode voltages. It shows the existence of anode sheath where most of the anode potential is dropped and only a small fraction penetrates within the plasma. A little rise in the floating potential within the plasma is not understood. As in the low resistance mode, there is practically no variation of floating potential along the axis, shown in figure 5.

This mode of operation is further divided in two subgroups, e.g., high pressure mode and low pressure mode as described by Roth (1976) in connection with the Bumpy Torus plasma.

The high pressure mode occurs at lower anode voltage and above certain threshold pressure. This regime of operation is characterized by low electron temperature, usually up to 35 eV.

As the discharge voltage is increased, at a certain voltage a transition takes place following an oscillation in the discharge volume and the discharge current drops. After this the discharge current increases again with the discharge voltage but with a different rate. The transition from the high pressure to low pressure mode and vice versa becomes less prominent as the magnetic field is reduced. The plasma in the low pressure mode remains mainly confined in the midplane region, and is characterized by high electron temperature usually higher than 35 eV. As the anode voltage is increased, a bright hollow plasma column (a plasma ring if viewed from the end) is formed which becomes brighter and pushed more near the axis as the anode voltage is increased. Figure 7 shows an end-view photograph of the column which was taken at a pressure of  $1.8 \times 10^{-5}$  torr, anode voltage of 23.5 kV and a magnetic field of 6.5 K gauss at the mirror throat. Increase of magnetic field makes the column more confined and a reduction of it makes the column diffused.

Figure 8 shows the floating potential distribution of the high resistance mode as a function of anode voltage taken at a position midway between the throat and the midplane. It is seen that a sharp transition in the floating potential occurs around  $V_a = 10$  kV.

#### (c) Transition Mode

In between the high resistance and low resistance modes there exists a transition mode whose property is quite different from the others. In this mode the discharge voltage and the discharge current are high and increase of discharge voltage finally leads to current saturation. The

electron velocity distribution in this case is prominently non-Maxwellian. (The non-Maxwellian property of the plasma was evident from the nonlinearity of the Langmuir probe characteristic even in the transition region.) Also there exists a potential drop from the throat to the midplane which in most cases is nonmonotonic as shown in figure 9. Figure 10 shows the radial floating potential distribution in the mirror throat region for a given anode voltage. The floating potential distribution in the transition mode remains almost constant for a wide variation of pressure (not shown here). The same figure 10 shows the corresponding floating potential distributions in the low and high resistance modes.

### RF Probe Measurements

Figure 11 shows a typical plot of probe resistance  $R_t$  and reactance  $x_t$  plotted against the probe bias voltage, where,

$$R_t - jx_t = (R_1 - jx_1) + (R_2 - jx_2)$$

$R_1 - jx_1$  and  $R_2 - jx_2$  being the rf impedances of the probe sheath and the presheath (disturbed plasma region lying between sheath and undisturbed plasma) regions, respectively. As the probe bias voltage was gradually increased from the ion current region through the floating potential, the ion sheath was reduced, and consequently the values of  $R_1$  and  $x_1$ , until the space potential is reached when  $R_1 = x_1 = 0$ . This is marked by  $V_s$  in the figure after which the electron sheath is formed. It can be argued that the impedance of the presheath remains practically constant during the operation.<sup>10</sup> (Sen and Basu, 1973)

Eliminating the effect of the presheath, the local values of the electron density and electron temperature can be calculated, the details of which has been published elsewhere<sup>13</sup> (Sen, Ph.D. Thesis, 1973). Table I shows the values of  $T_e$  and  $n_e$  for different values of the discharge current, discharge voltage, pressure, and magnetic field. Due to the limitations of the present experimental set up, a systematic parametric variation could not be made.

### DISCUSSIONS AND CONCLUSIONS

The modified Penning discharge has been operated over a wide range of experimental parameters in which the discharge was shown to undergo different mode transitions. The amount of potential the plasma could sustain in different modes is different. In the high resistance mode, for example, the plasma is shielded by the anode sheath where most of the anode potential drops and only a small fraction of it penetrates within the plasma (fig. 6). The plasma in the low resistance mode, on the other hand, floats at a considerable fraction of the anode voltage (fig. 4). The sharp sheath structure is also absent in the transition mode (fig. 10)

which like the high resistance mode could be operated at high discharge voltages. The transition mode is also characterized by having an axial potential drop from the mirror throat to the midplane, which also may not be monotonic (fig. 9). This is not true for the low and high pressure modes of operation where there is practically uniform potential along the axis.

The study of the floating potential distribution in the modified Penning discharge is only one step forward in understanding the particle transport phenomenon. For a better understanding of the problem, a simultaneous measurement of the distributions of the electron density and electron temperature is necessary which has not been done in the present study.

The electron temperature and the electron density measured by the rf impedance probe agrees very well with the corresponding d.c. probe data in the glow and arc discharges in absence of a magnetic field. In the case of the modified Penning discharge where a strong magnetic field is present, the results do not agree so well. Although the agreement between the rf and d.c. values of electron temperature agree fairly well at low magnetic fields, it becomes poorer as the magnetic field is increased, the value of  $T_e$  (DC) being always higher. Similar effect has been observed by Chen et al.<sup>14</sup> (1968) where they observed in probe measurement an increase of  $T_e$  by 30 percent in presence of a magnetic field. Although they were not definite about the cause, it was suggested that magnetic field might be one of the possible reasons. In this present study the disagreement of  $T_e$  becomes more as the magnetic field is increased might suggest that the magnetic field is playing a part in determining  $T_e$  by d.c. methods.  $T_e$  was measured from the transition part of the probe characteristic (Brown et al., 1971).

The disagreement of the values of the electron density by the two methods is quite high,  $n_e$  (RF) being 50 to 60 times the value of  $n_e$  (DC). This is the case even where  $T_e$  (RF) and  $T_e$  (DC) agree quite well. This result is, of course, somewhat expected because: (1) The saturation electron current to a disc probe always reduces in the presence of a magnetic field even when its plane is perpendicular to it<sup>16</sup> (Dote et al., 1966). In fact  $I_{e11}/I_0$  (where  $I_0$  is the saturation electron current in absence of a magnetic field) tends to zero as  $\omega\tau$  approaches infinity, where  $\omega$  is the electron cyclotron frequency and  $\tau$  is the mean collision time between electron and neutral particles. (2) The large probe area used for rf measurement may cause excessive electron depletion in front of the probe surface leading to a reduction of the probe current.

The minima in the  $R_t$  and  $x_t$  curves of probe impedance may serve as an indication for the space potential, which is poorly located by the d.c. methods and is more meaningful than floating potentials. The limitation of the present experimental set-up for rf measurement did not permit a parametric study to be made using the impedance probe. Improvement of the measuring system and comparison of the rf results with an independent diagnostic data may prove that the rf impedance probe technique is a useful method for studying magnetized plasma.

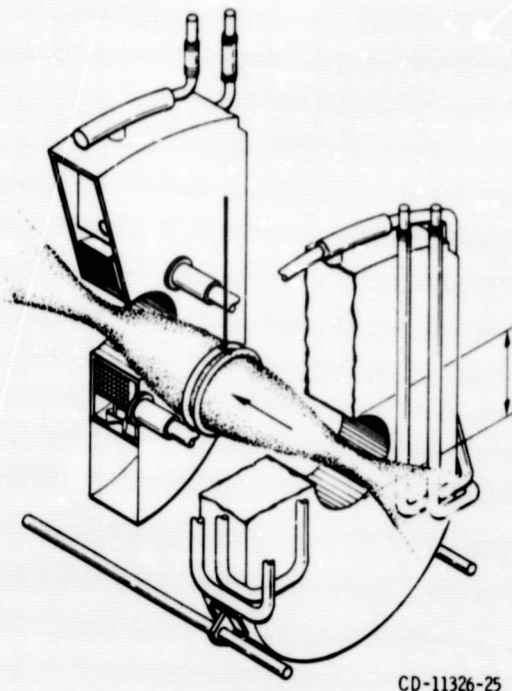


## REFERENCES

1. J. R. Roth, Rev. Sci. Instrum. 37, 1100 (1966).
2. J. R. Roth, IEEE Trans. Plasma Sci. PS-1, 34 (1973).
3. J. R. Roth and M. Clark, Plasma Phys. 11, 131 (1969).
4. J. R. Roth, Plasma Phys. 15, 995 (1973).
5. J. R. Roth, Phys. Fluids 14, 2193 (1971).
6. J. R. Roth, Phys. Fluids 16, 231 (1973).
7. F. C. Jobs and R. L. Hickok, Nucl. Fusion 10, 195 (1970).
8. J. R. Roth, G. A. Gerdin, and R. W. Richardson, NASA TN D-8114 (1976).
9. Y. Nishida and A. Hirose, 1976 IEEE Int. Conf. on Plasma Sci., Austin, Texas (1976).
10. C. Sen and J. Basu, J. Phys. D: Appl. Phys. 6, 172 (1973).
11. J. Basu and C. Sen, J. Appl. Phys. 46, 2298 (1975).
12. J. Basu and C. Sen, Proc. IEEE 55, 1767 (1967).
13. C. Sen, Ph.D. Thesis, Calcutta Univ. (1973).
14. F. F. Chen, C. Etievant, and D. Mosher, Phys. Fluids 11, 811 (1968).
15. I. G. Brown, A. B. Compher, and W. B. Kunkel, Phys. Fluids 16, 1377 (1971).
16. T. Dote, H. Amemiya, and T. Ichimiya, Jap. J. Appl. Phys. 3, 789 (1966).

TABLE I

P (Torr)	B <sub>max</sub> (K Gauss)	V <sub>D</sub> (KV)	I <sub>D</sub> (A)	T <sub>e</sub> (eV)		n <sub>e</sub> (×10 <sup>14</sup> /m <sup>3</sup> )	
				RF	DC	RF	DC
1.24×10 <sup>-4</sup>	4.2	1.6	0.016	14.2	16.7	11.0	0.20
4.2×10 <sup>-5</sup>	4.2	7.5	.0108	19.4	19.0	20.1	.56
1.7×10 <sup>-4</sup>	6.5	1.2	.0148	9.7	15.8	2.2	.13
1.6×10 <sup>-4</sup>	9.9	1.4	.026	8.9	14.8	6.7	.16
1.3×10 <sup>-4</sup>	11.2	2.0	.037	12.5	26.0	8.0	.25



CD-11326-25

Figure 1. - Isometric cutaway drawing of a modified penning discharge.

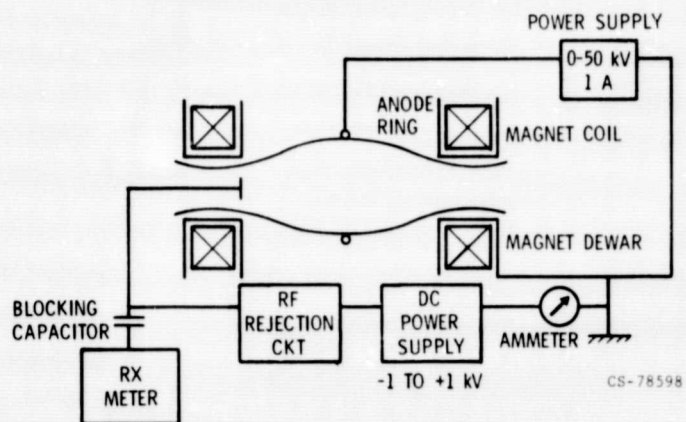


Figure 2. - Block diagram of the probe impedance measuring system.

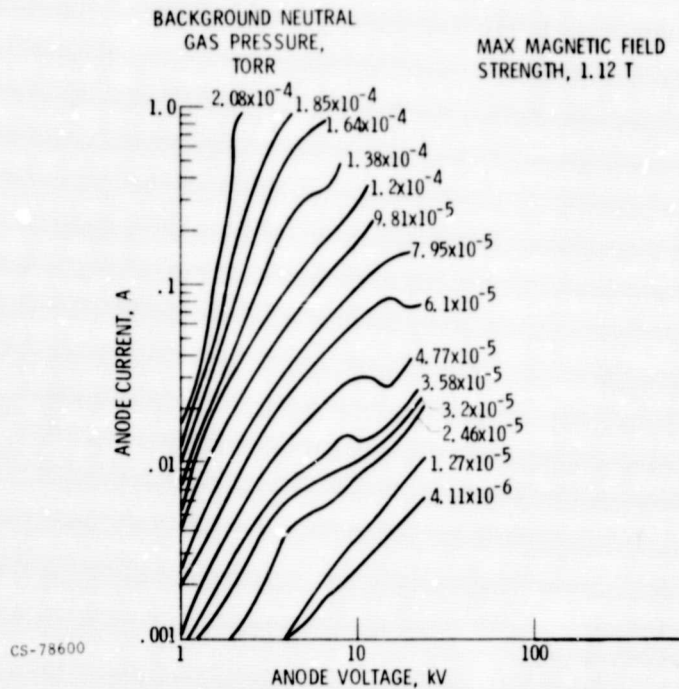


Figure 3. - I - V characteristic curve of a modified Penning discharge.

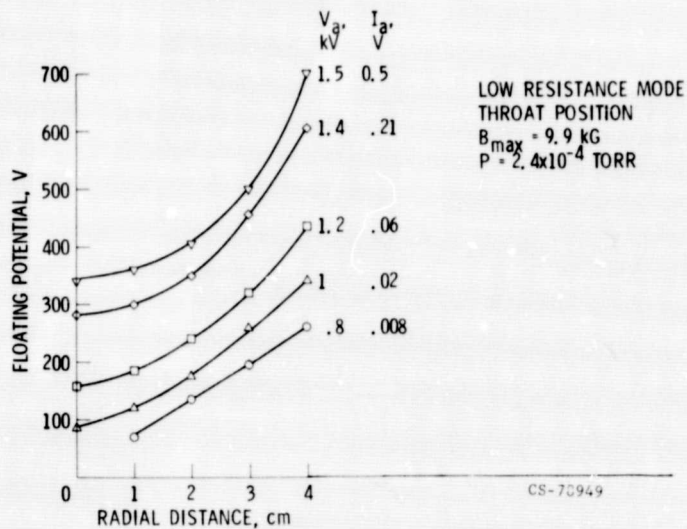


Figure 4. - Radial floating potential distribution in the low resistance mode taken at the mirror throat position.

ORIGINAL PAGE IS  
OF POOR QUALITY



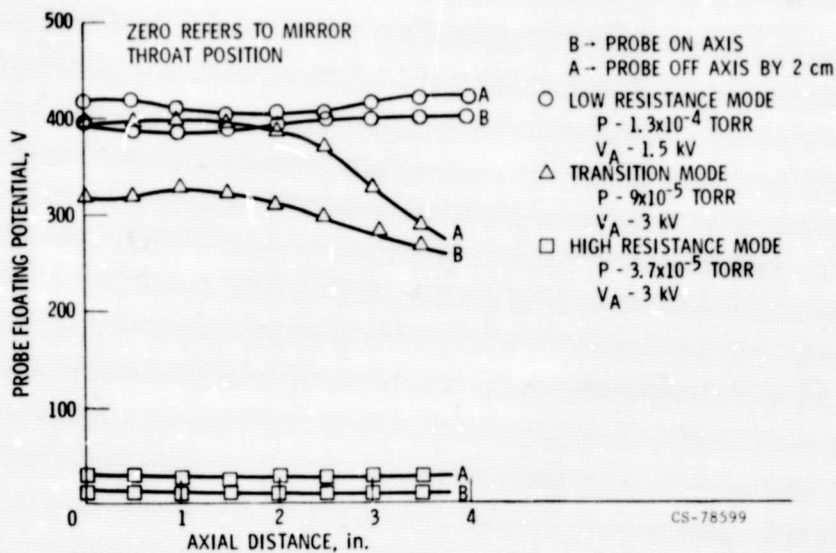


Figure 5. - Axial floating potential distribution for different modes.

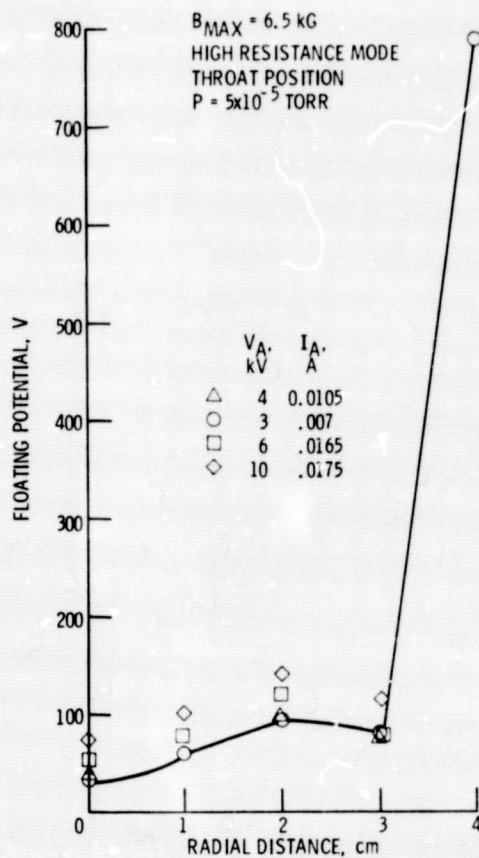


Figure 6. - Radial floating potential distribution for the high resistance mode.

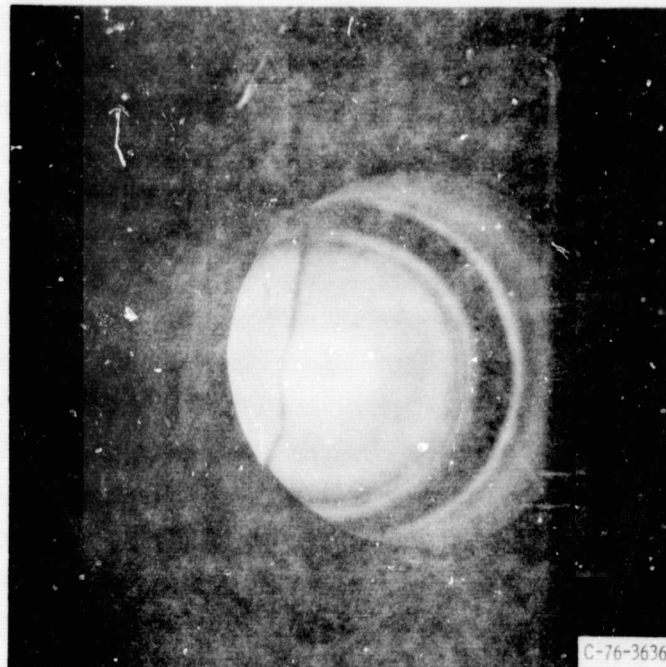


Figure 7. - End view of hollow plasma column formed in high resistance mode.

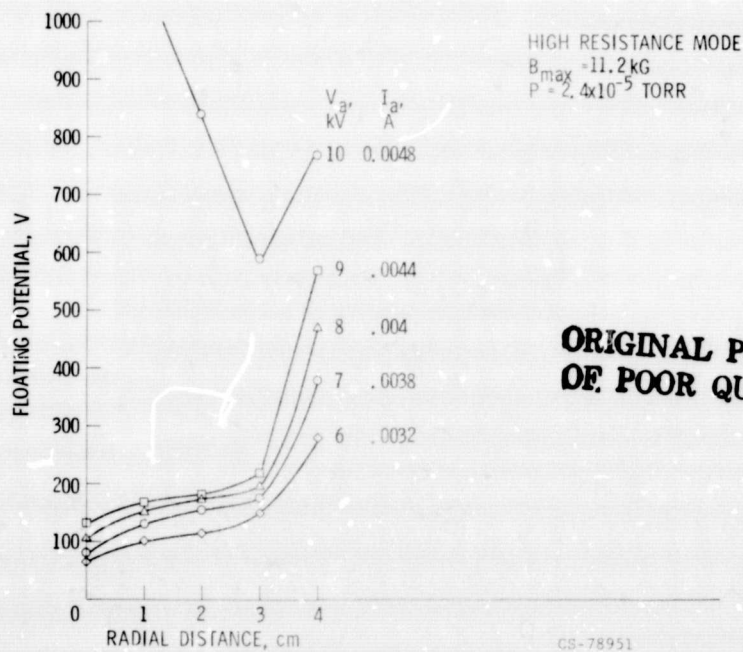
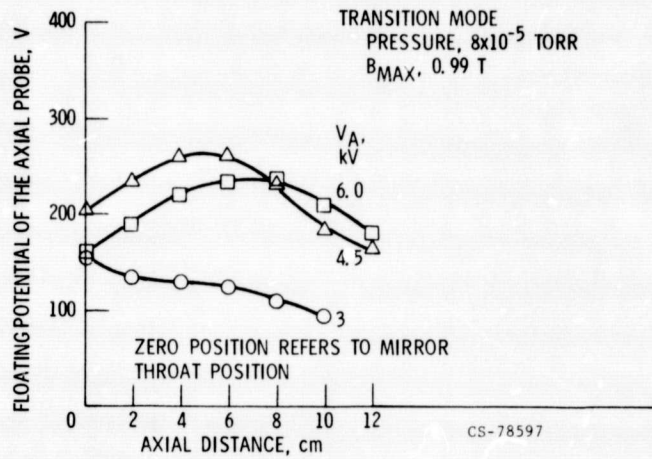


Figure 8. - Radial floating potential distribution in the high resistance mode, taken at a position 6 cm inside from the mirror throat.

**ORIGINAL PAGE IS  
OF POOR QUALITY**



ORIGINAL PAGE IS  
OF POOR QUALITY

Figure 9. - Axial floating potential distribution in the transition mode for different anode voltages.

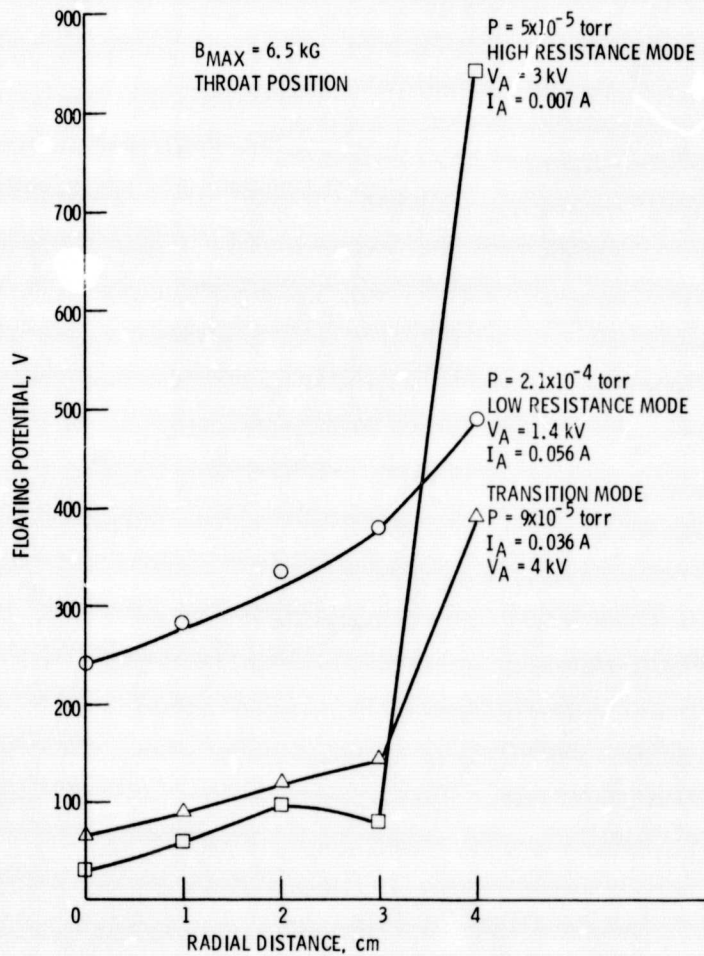
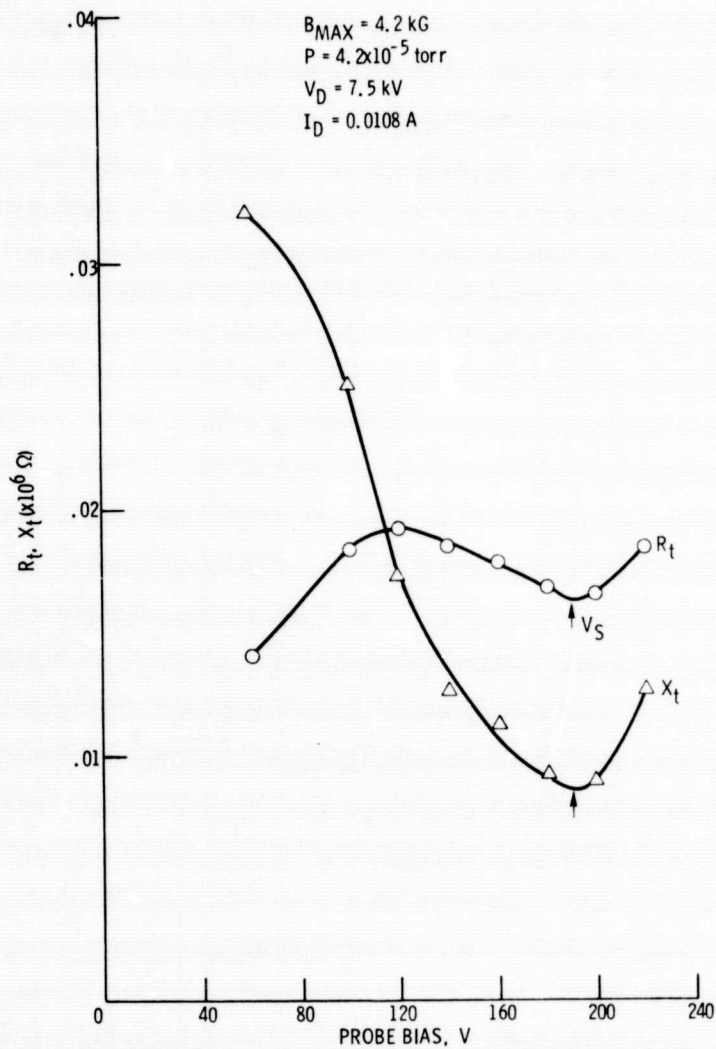


Figure 10. - Radial floating potential distribution for three modes.



ORIGINAL PAGE IS  
OF POOR QUALITY

Figure 11. - Typical plot of probe resistance and reactance against bias voltage.